

Stability of non-homogeneous models and fine tuning of initial state

P. Sundell and I. Vilja

Department of Physics and Astronomy, University of Turku, FI-20014 Turku, Finland

(Dated: June 15, 2021)

We apply phase space analysis to inhomogeneous cosmological model given by Lemaître-Tolman model. We describe some general conditions required to interpret the model stable enough and, in the present paper, apply them to two special cases: dust filled homogeneous model with and without cosmological constant. We find that such stability explaining all present astrophysical observations can not be achieved due to instabilities in phase space. This hints that non-homogeneous models are not likely to be physically viable, although any conclusive analysis requires more realistic modeling of non-homogeneous universe.

I. INTRODUCTION

Supernovae observations^{1,2} made just before the break of the millennium implies that the universe appears to be expanding at an increasing rate. A bit later made observations of cosmic microwave background (CMB) radiation³ supports the conclusions made out of the supernovae observations. The most popular ways of explaining these observations are with models based on Friedmann-Lemaître-Robertson-Walker (FLRW) metric, which is based on general relativity and the principles of cosmological and Copernican. The cosmological principle merely states that the universe is spatially homogeneous everywhere, whereas the Copernican principle states that there are no preferred points in the universe. FLRW metric and models based on it are extensively presented in the literature of cosmology (see for example⁴).

Even though the FLRW based models fit well inside the frame provided by our observations, it is also for long known to suffer some problems, for example the fine tuning problem^{4,5} and the cosmological constant problem^{4,6}. One of the strengths of the FLRW based models is simplicity due to various approximations, although, that can also be counted as a weakness. It is also questionable if all approximations are made acceptably, as is pointed out by Shirokov and Fisher⁷, where is questioned if the homogeneity approximation should be done to the Einstein tensor $G_{\mu\nu}$, rather than to the metric $g_{\mu\nu}$, since in general $\langle G_{\mu\nu}(g_{\mu\nu}) \rangle \neq G_{\mu\nu}(\langle g_{\mu\nu} \rangle)$. However, the problem is more complex than this. As pointed out by Shirokov and Fisher⁷, Einstein equations are no longer tensor equations after averaging in the sense, that they can not be changed *e.g.* from covariant form to contravariant form with metric tensor without altering the equations. In this perspective it seems, that only tensors rank 0 and scalars have well validated averages. For this kind of approach see Buchert⁸, where he transforms the Einstein equations into scalar equations before averaging. It is very much possible that the problems FLRW based models suffer are due to approximations, and solely the work of Shirokov, Fisher and Buchert implies that the first approximation to investigate more is the homogeneity. Such a model was first introduced by Lemaître⁹, and later on studied by Tolman¹⁰ and its called Lemaître-Tolman (LT) model. For further developments of the model see^{11,12}. The LT model have not yet been studied as widely as FLRW based models, hence all the problems it suffers have probably not yet been discovered, but it have already shown its power by overcoming some of the problems of the FLRW based models. For example, Mattsson has shown that the LT model can explain the main cosmological observations without dark energy.¹⁴

Actually, FLRW based models are often presented including early times inflation, which solves the fine tuning problem. This solution can not be generalized to LT model *a priori*, because the evolution of the universe in LT model is dependent in coordinate distance, which would make the inflation occur differently in separate locations, and the consequences of this are unknown. However, inflation is not the only possible explanation for the homogeneous tendency of cosmological observations. We explore the possibility that the structure of the equations governing the evolution of the universe is such, that it has a inbuilt property to make everything appear as observed. We study the existence of this property by using phase space analysis. The aim is to find restrictions to viable and stable solutions of the differential equations governing the universe in the LT model. Viable solutions mean here that the solutions are consistent with the observations. Stable solutions include such solutions, which are attracted towards the universe we observe; therefore these kind of solutions do not need fine tuning of initial state. Especially interesting cases are where the dark energy is absent.

It is also interesting to see, if our results offers insight to the homogeneity approximation. By that we mean, if all the viable and stable LT models are approximately homogeneous. This subject however is not going to be important in this paper, but it is merely pointed out as a possibility what more can our results offer.

The focus of the present paper is to introduce a novel method to use stability analysis and its general features with the Lemaître-Tolman model, which is done in section II. In section IIA, homogeneous cases in general are applied to the methods found out. In sections IIB and IIC pressure free, flat and homogeneous universe is investigated, in the

cases of dust filled and dust and dark energy filled universes, using the phase space analysis. Finally in section III the results are discussed. Realistic applications where viable and stable inhomogeneous models are to be determined are left to forthcoming publications.

II. LEMAÎTRE-TOLMAN MODEL AND PHASE SPACE ANALYSIS

The LT model¹² describes a dust filled inhomogeneous but isotropic universe which energy momentum tensor reads as $T^{\mu\nu} = \rho u^\mu u^\nu$.²¹ Here $\rho = \rho(t, r)$ is matter density and u^μ is the local four-velocity. As the coordinates are assumed to be comoving, the four-velocity is simply $u^\mu = \delta_t^\mu$. The standard synchronous gauge metric in the LT model is given by²²

$$ds^2 = -dt^2 + \frac{R_r^2 dr^2}{1+f(r)} + R(t, r)^2 (d\theta^2 + \sin^2 \theta d\phi^2), \quad (1)$$

where the subscript r denotes derivative with respect to radial coordinate, $R_r = \partial R(t, r)/\partial r$, and $f(r) > -1$. In this prescription the evolution of universe is built in to the local scale factor R whereas function f controls the overall radial dilatation. Including the cosmological constant Λ into the Einstein equations, after some integrations, one obtains the relevant differential equations as

$$\dot{R}^2 = \frac{2M}{R} + f + \frac{\Lambda}{3}R^2, \quad (2)$$

and

$$\kappa\rho = \frac{2M_r}{R_r R^2}, \quad (3)$$

where $M = M(r)$ is a arbitrary function, $\kappa = 8\pi G/c^4$, and G is the Newton's constant of gravity.

In general, all the quantities (or functions) in Eqs. (2) and (3) are unknown. However, if they are presented as quantities dependent only on redshift, they can be received from cosmological observations, or be derived from the observations, *e.g.* if $R(z)$ is known we get $R_z(z)$ as its derivative. In the LT models the redshift equation reads as

$$\frac{dz}{dr} = \frac{(1+z)R_{rt}(r, t)}{\sqrt{1+f}}, \quad (4)$$

and the angular diameter distance d_a is $d_a(z) = R(t(z), r(z))$.¹³⁻¹⁵

The relation between t and r can be given as follows. The path of radial light ray is given by the radial null geodesic, where $ds^2 = d\theta^2 = d\psi^2 = 0$. Using metric (1) it is

$$dt = \pm \frac{R_r}{\sqrt{1+f}} dr, \quad (5)$$

where the signs correspond an incoming (-) and an outgoing (+) light rays. It is possible¹⁶ to choose radial coordinate r , *i.e.* use remaining gauge freedom so, that for incoming ray $dr = -dt$. So, along the ray

$$t = t(r) = t_0 - r, \quad (6)$$

where $t = t_0$ refers to present time. For any quantity, a hat $\hat{}$ denotes that it is evaluated along (incoming) light ray, *e.g.* $\hat{R} = R(t(r), r)$. Thus, the gauge condition for Eq. (6) for incoming light can be written as

$$1 = \frac{\hat{R}_r}{\sqrt{1+f}}. \quad (7)$$

On the radial null geodesic it can be shown¹⁶ that the relation between the matter density $\rho(t, r)$ and the number density of light sources in redshift distance²³ $n = n(z)$ is given by

$$\hat{\rho} = \frac{\mu n}{\hat{R}^2} \frac{dz}{dr}, \quad (8)$$

where $\mu = \mu(z)$ is the mean mass per source at given redshift distance. After some manipulation, using Eqs. (2), (3), (6), (7), and (8) the redshift equation (4) can be cast in the form¹⁶

$$J(z)z_r + K(z)z_r^2 + L(z)z_{rr} = 0, \quad (9)$$

where we have defined²⁴

$$\begin{aligned} J(z) &= \kappa(1+z)\mu n, \\ K(z) &= 2R[R_z + (1+z)R_{zz}], \\ L(z) &= 2(1+z)RR_z. \end{aligned} \quad (10)$$

All the quantities in Equations J , K , and L are only dependent on redshift z , and they are all measurable or they can be derived from measurable quantities. Moreover, because it is evident that the quantities dependent only on redshift are evaluated along light ray, every function or quantity dependent only on z is presented without a hat. Especially now $R = R(z) = \hat{R}(t(r(z)), r(z))$, and hence $R_z = \partial R(z)/\partial z = dR(z)/dz$ and $R_{zz} = \partial^2 R(z)/\partial z^2 = d^2 R(z)/dz^2$. Eq. (9) is a second order non-linear differential equation, from which can be solved z as a function of r . However, that is not the interest here, but rather investigating the stability of different solutions. We use phase space analysis^{17,18} for investigation. Here is chosen $z_r = y$ to give

$$\begin{cases} y_r = -y \frac{J(z)+K(z)y}{L(z)} \\ z_r = y. \end{cases} \quad (11)$$

Note, that we have given the redshift in terms determined comoving coordinate r , which is related along the ray to time as $r = t_0 - t$. This means that we can use practically interchangeably the two parameter r or t .

Analyzing cosmological data will give us functions J , K , and L explicitly with respect to z , but even now when the explicit forms are unknown, general remarks can be done on what kind of systems Eq. (9) can describe. The phase plane can be divided into sections each having its own characteristics. Some of the properties can be read out from general properties of the equations and represented as a flow plot in zy -plane.

The y -axis represents location of observations (Earth) at present time; the redshift is there zero. On the right hand side of the y -axis is past or distant objects and the left hand side of the y -axis can be interpreted as future. On the z -axis $z_r = z_t = 0$, hence it represents apparently static universe. Above the z -axis $z_r > 0$, the area represents apparently (and locally) expanding space, and below the z -axis $z_r < 0$ the apparently contracting one. Therefore, due to the observations, we are mostly interested of the first quarter of a phase space plane, past of an expanding universe; however, we do not want to exclude other parts of the phase plane *per se*, but we give the first quarter of the phase space plane most of our interest.

Looking to the latter of the Eqs. (11) one sees, that whenever $y > 0$ the flow arrows points right, and when $y < 0$ they points left. The curves where y_r or z_r is zero are called nullclines and the points where y_r and z_r is zero are called fixed points. In the system (11) all the points on curve $y = 0$ are fixed points, which means that the curve $y = 0$ is fixed. The curves where $L(z) = 0$ needs special attention as the system (11) is not well defined there. The physical perspective also gives more restrictions. The form of function J reveals that it is positive implying that the curve $J(z) + K(z)y = 0$ can not cross the z -axis. The only exceptions are at the origin of the spherical symmetry ($r = 0$), where it is required to have $R(t, 0) = 0$ for all t to avoid point mass and curvature singularity at $r = 0$, and possibly at the Big Bang or the Big Crunch.¹² Requirement $R(t, 0) = 0$ in gauge (6) is $R(t_0, 0) = 0$, which is compatible with $R(z)$ being zero at $z = 0$ as $R(z)$ is the angular diameter distance. Because J is always positive (neglecting the special points discussed above) and K and L seem to able to change their signs, combining these functions with different allowed signs there is essentially four different types of situations (in the case of system (11)) that can appear on the phase portraits, presented in Fig. 1. The nature of the function $R(z)$ implies that L is zero only if $R_z(z)$ is zero (neglecting again the special points discussed above) and because $R_z(z) = R_r(r)r_z$, is then either $R_r(r)$ or r_z zero. The latter case can approach to zero when $y \rightarrow \infty$, and $R_r(r) = 0$ occurs at the apparent horizon¹⁶.

Consider now the situation where functions J , K , and L are formed from observational data. Eq. (11) is now given explicitly, so phase plane can be drawn and the best fit curve compared to observations can be fitted. It is assumable that the best fit curve coincides closely to the best fit to the observations in the isotropic and homogeneous models, which means that the best fit curve is not very "lumpy" and is approximately monotonic. Now, consider each observable separately. Each of them have their own trajectory, which are unknown to us, because we do not have enough data from each observable. But if we had enough data from each observable, we could draw their trajectories on the same phase plane that the best fit curve is on. So, each observable have their own trajectory, but still they seem to sit on a approximately monotonic curve, the best fit curve. In our scheme this appears to happen only, if the flow arrows are pointing towards the best fit curve. This would ensure that for large number of initial values,

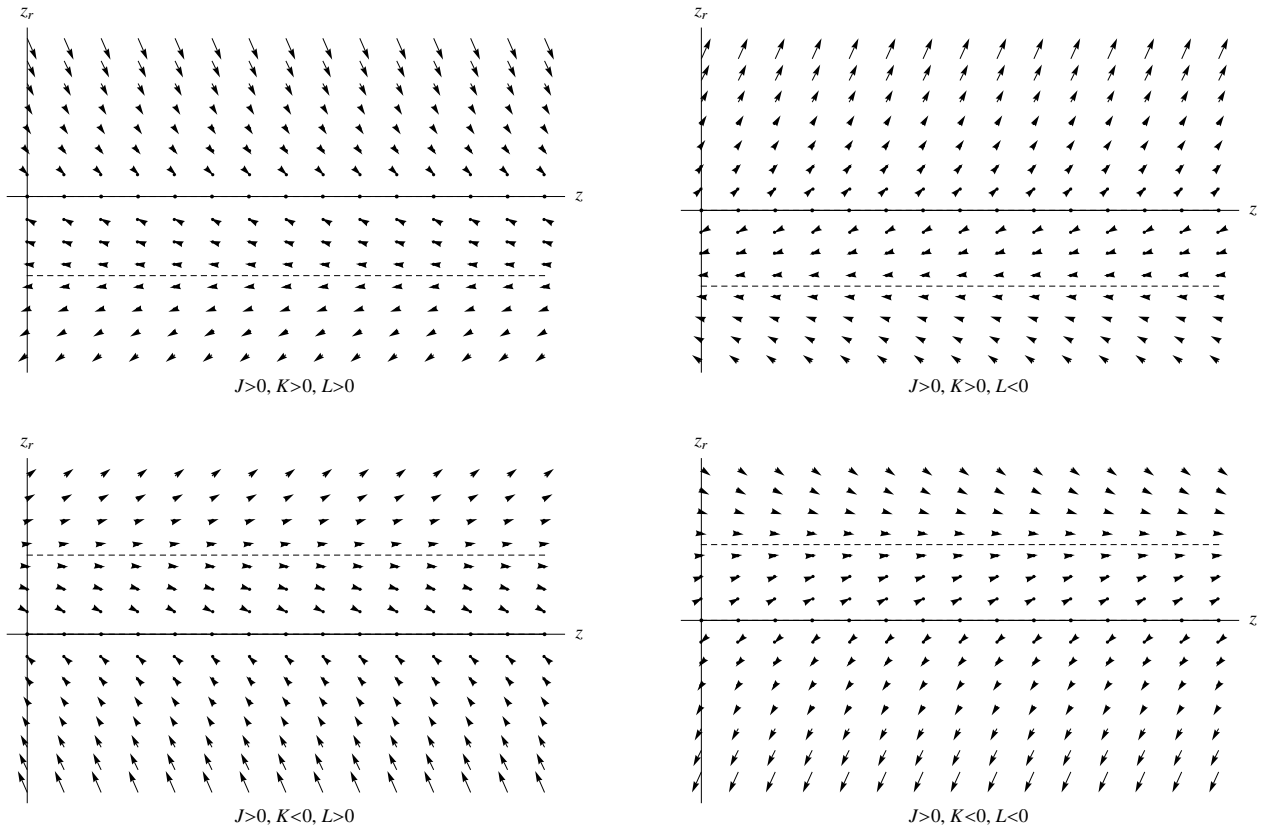


FIG. 1: Four different situations depending on the signs of K and L that can occur on a phase plane with the system (11). Functions J , K , and L are here chosen to be $+1$ or -1 for simplicity. The dashed curve is the nullcline $J + Ky = 0$.

observables end up (after long enough time period) near by to the best fit curve. This issue, however, is not that simple and it will be discussed more in section Conclusions and discussion.

At simplest the interest in phase plane analysis is concentrated into the existence and properties of the fixed points. In this case however, observations suggests that the best fit curve should be attractive. In the system (11) only z -axis can be referred as a attractive curve, but its nature as apparent static universe is not what is observed. However, nullclines can be thought of to be attractive like, since flow arrows can point towards them as in *e.g.* the low-right case in Fig. 1. In our system the only physically interesting possible attractive like nullcline is $J(z) + K(z)y = 0$. However, the exact identification between the nullcline and the best fit curve can not be done, because then both Eqs. $J + Ky = 0$ and (9) should be satisfied simultaneously causing either the solution $y(z)$ be linear or $L(z) = 0$, but it is not even necessary as long as the identification can satisfy observations inside their inaccuracy limits.

The properties of the system (11) discussed above implies that the curve $J + Ky = 0$ can be attractive in the first quarter of the phase plane only if J is positive and K and L are negative. Even though these boundaries are necessary, they are far from sufficient for the following reason. Consider a situations where $0 < J$, and $K, L < 0$ and the value of the slope of the curve $J + Ky = 0$, $-J/K$, is positive. On the curve $J + Ky = 0$ is always $y_r = 0$, thus flow arrows on the curve are horizontal and pointing right, *i.e.*, the slopes of the flow arrows $y_z = y_r/z_r$ are zero. Now, approaching the curve from below vertically makes y_z to approach zero. At some distance to $J + Ky = 0$ before y_z reaches to zero, it becomes smaller than $-J/K$. This means that the solution is no longer approaching the curve $J + Ky = 0$, because flow arrows determine the slopes and the progressing directions of the solutions in each point. Similar situation occur, if at fixed z we approach the curve $J + Ky = 0$ from above and $-J/K < 0$. This is also why nullclines are rather attractive like than attractive. As it follows, we need more sufficient methods to measure the attractivity of the nullcline $J + Ky = 0$. Especially, we need a method to measure the distance from the nullcline where it stops acting as an attractor. In the present paper for this is used the following method.

Let us consider our system on area $z, y > 0$ with positive J and negative K and L . The nullcline $J(z) + K(z)y = 0$ is attractive like, if flow arrows around it points towards it. Now below the nullcline flow arrows point up-right and above the curve they point down-right. The slope of the nullcline is positive and all the flow arrows above it points

towards it, but the flow arrows below it points towards it only if the slopes of the flow arrows $y_z(z)$ at some given z are greater than the slope of the nullcline $-J/K$ at the same z . Let $\delta_y > 0$ be the (vertical) distance from the nullcline $J(z) + K(z)y = 0$. The slope of the flow arrow at given z and distance δ_y below the nullcline is:

$$\begin{aligned}
y_z^- &:= \left[\frac{(y - \delta_y)r}{z_r} \right]_{y=-J(z)/K(z)} \\
&= \left[\frac{-(y - \delta_y) \frac{J(z) + K(z)(y + \delta_y)}{L(z)}}{y - \delta_y} \right]_{y=-J(z)/K(z)} \\
&= - \left[\frac{J(z) + K(z)(y - \delta_y)}{L(z)} \right]_{y=-J(z)/K(z)} \\
&= \frac{K(z)\delta_y}{L(z)} - \left[\frac{J(z) + K(z)y}{L(z)} \right]_{y=-J(z)/K(z)} \\
&= \frac{K(z)}{L(z)} \delta_y.
\end{aligned} \tag{12}$$

From Eq. (12) one can explicitly see, that the size of the vertical step δ_y taken from the nullcline effects to the attractiveness in a linear fashion: the larger the step is, more attractive like the nullcline seems. This means that δ_y takes a role of a parameter comparable to observational inaccuracies. Hence, the slopes of the flow arrows $y_z(z)$ are greater than the slope of the nullcline $-J/K$ at at some given z , if

$$\frac{K(z)}{L(z)} \delta_y > y_z = -\frac{J_z(z)}{K(z)} + \frac{J(z)}{K(z)^2} K_z(z). \tag{13}$$

The above inequality is the restriction we use to study the attractiveness of the nullcline $J + Ky = 0$.

A. Isotropic and homogeneous models

To give more concrete touch of our prescription, we check how the method works with isotropic and homogeneous models. Note, that FLRW metric can not be used here, because it is not compatible with our gauge choice $dt = -dr$. This can be explicitly seen by comparing the standard FLRW metric relation between r and z given by⁴

$$r = \frac{2z\Omega_0 + (2\Omega_0 - 4)(\sqrt{z\Omega_0 + 1} - 1)}{a_0 H_0 (z + 1) \Omega_0^2}, \tag{14}$$

with $a = a_0/(1 + z)$ to the relation derived from Eq. (7), $a = \sqrt{1 - kr^2}$ giving

$$r = \pm \sqrt{\frac{1}{k} - \frac{a_0^2}{k(1 + z)^2}}. \tag{15}$$

Clearly Eqs. (14) and (15) are not equivalent, except in some special cases. However, it is necessary to write isotropic and homogenous space-time in Robertson-Walker coordinates, and we can proceed by other means.

In spherically symmetric homogeneous space-time the metric can always be given as¹⁹

$$ds^2 = g(v)dv^2 + f(v) \left(d\mathbf{u}^2 + \frac{k(\mathbf{u} \cdot d\mathbf{u})^2}{1 - k\mathbf{u}^2} \right), \tag{16}$$

where v and $\mathbf{u} = (u_1, u_2, u_3)$ are the coordinates, $g(v)$ is a negative and $f(v)$ is a positive function of v , and k is spatial curvature and can be chosen to be 1, 0, or -1. For our purposes it is convenient to define new coordinates t , r , θ , and φ by

$$\begin{aligned}
\sqrt{-g(v)}dv &= dt, \\
u_1 &= \Theta(r) \sin \theta \cos \varphi, \\
u_2 &= \Theta(r) \sin \theta \sin \varphi, \\
u_3 &= \Theta(r) \cos \theta.
\end{aligned} \tag{17}$$

Then we have

$$ds^2 = -dt^2 + a^2(t) \left[\frac{\Theta_r^2}{1 - k\Theta^2} dr^2 + \Theta^2 d\Omega^2 \right], \quad (18)$$

where $a(t) = \sqrt{f(v)}$ and $d\Omega^2 = d\theta^2 + \sin^2\theta d\varphi^2$. With the above metric definition the field equations take the normal Friedmann form and therefore can be written as

$$a_t = H_0 a \sqrt{\sum_i \Omega_i^{(0)} (a/a_0)^{-3(1+w_i)}}, \quad (19)$$

where $\Omega_i^{(0)}$ is the present value of the energy density of different energy forms. For dust, dark energy, and spatial curvature, the w_i takes values 0, -1 , and $-1/3$ respectively. Because the LT model does not take pressure into account, for our purposes it is unnecessary to include relativistic matter here either, even though generally it could be done.

To be able to use the Eqs. (11), we need to specify quantities μ , n and R . According to Eq. (8), μ and n can be given with R , ρ , and z_r , and because in metric (18) $R = a\Theta$, we need to find out presentations for quantities a , Θ , ρ , and z_r with respect to z .

In LT model, the energy momentum tensor $T^{\mu\nu}$ includes only dust, hence

$$\rho = \rho^{(0)} (a_0/a)^3, \quad (20)$$

where $\rho^{(0)} = \Omega_M^{(0)} \frac{3H_0^2}{\kappa}$, and $\Omega_M^{(0)}$ is the present dust (or non-relativistic matter) density of the universe.

With metric (18) equations (7) and (4) reduces to be

$$1 = \frac{a\Theta_r}{\sqrt{1 - k\Theta^2}} \quad (21)$$

and

$$\frac{dz}{dr} = \frac{(1+z)a_t\Theta_r}{\sqrt{1 - k\Theta^2}}. \quad (22)$$

Combining these the usual Robertson-Walker relation

$$\frac{1}{1+z} = \frac{a}{a_0} \quad (23)$$

is reproduced and as $r = t_0 - t$ is $z_r = a_0 a_t / a^2$, we can write

$$z_r = H_0 (z+1) \sqrt{\sum_i \Omega_i^{(0)} (z+1)^{3(1+w_i)}}. \quad (24)$$

In the given gauge, the function Θ can be calculated directly from Eq. (21), which can also be written as

$$\int_{\Theta_0}^{\Theta} \frac{d\Theta}{\sqrt{1 - k\Theta^2}} = \int_0^z \frac{1+z}{a_0} \frac{1}{z_r} dz, \quad (25)$$

where we have used the relation

$$\int_0^r \frac{dr}{a} = \int_0^z \frac{1}{a} \frac{dr}{dz} dz = \int_0^z \frac{1+z}{a_0} \frac{1}{z_r} dz. \quad (26)$$

$\Theta(r=0) = 0$ is determined by the requirement $R(z=0) = 0$. The solution for curvature cases can now be integrated out. We find

$$\Theta = \sinh \left(\int_0^z \frac{1+z}{a_0} \frac{1}{z_r} dz \right), \quad k = -1, \quad (27)$$

$$\Theta = \int_0^z \frac{1+z}{a_0} \frac{1}{z_r} dz, \quad k = 0, \quad (28)$$

$$\Theta = \sin \left(\int_0^z \frac{1+z}{a_0} \frac{1}{z_r} dz \right), \quad k = 1. \quad (29)$$

In the following sections some numerical calculations are executed. To carry out the numerics we have chosen $100 \text{ km/s/Mpc} = 1$, which makes all the physical quantities dimensionless. For subsequent calculations also it is convenient to define a function

$$g := \frac{1}{H_0} \left[-\frac{J_z(z)}{K(z)} + \frac{J(z)}{K(z)^2} K_z(z) \right] \frac{L(z)}{K(z)}, \quad (30)$$

which in homogeneous models is $g = g(z; \Omega_i^0, a_0, H_0)$, *i.e.*, dependent on variable z and parameters Ω_i^0 , a_0 , and H_0 . Even further, it is easy to see, that in flat homogeneous cases $g = g(z; \Omega_i^0)$, thus the boundary condition (13) can be written as

$$\frac{\delta_y}{H_0} > g(z; \Omega_i^0). \quad (31)$$

The fact that $g(z; \Omega_i^0)$ do not include parameters a_0 , H_0 , or κ , considerably simplifies the boundary condition.

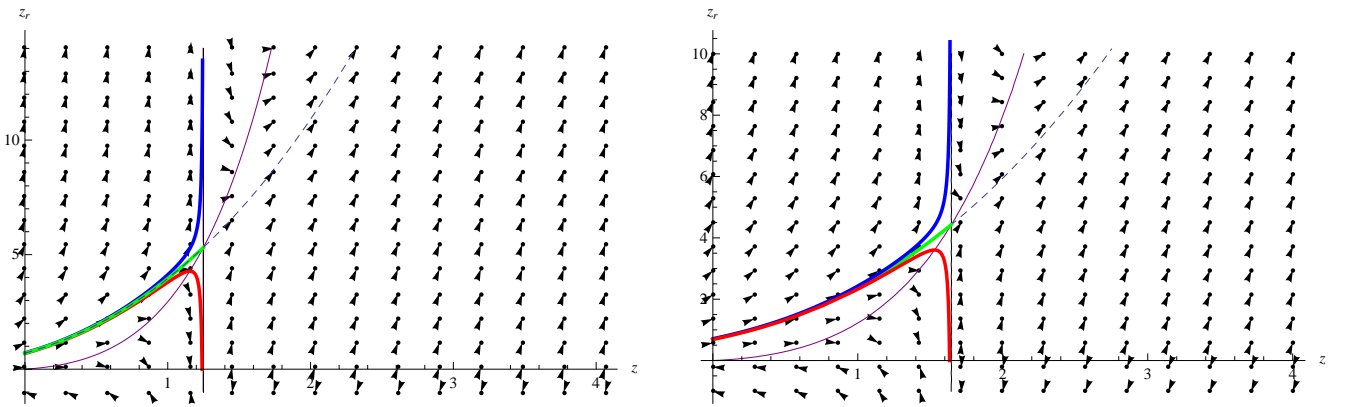


FIG. 2: Phase space portrait of the dust filled homogeneous universe (left hand side plane), when $H_0 = 0.70$, $\Omega_m = 1$, and $\Omega_\Lambda = 0$, and of the dust and dark energy filled homogeneous universe (right hand side plane), when $H_0 = 0.700$, $\Omega_m = 0.279$, and $\Omega_\Lambda = 0.721$. In both planes: thin purple curve is $J + Ky = 0$, thin black curve is $L = 0$, and red, green and blue thick curves are solutions of the system (11) with H_0 values 0.69, 0.70, and 0.71 respectively.

B. Dust filled universe

Let us study stability of the flat dust-filled homogeneous universe, which is often used approximation to investigate the evolution of the universe during matter dominated era. From Eq. (24) we obtain redshift relation

$$z_r = H_0(z+1) \sqrt{\Omega_m^{(0)}(1+z)^3}, \quad (32)$$

where $\Omega_m^{(0)} = 1$ is set from now on. The pair of differential equations (11) is now

$$y_r = \frac{y \left(y \left(9z - 4\sqrt{(z+1)^3 + 9} \right) - 6H_0(z+1)^2 \left(z(z+2) - \sqrt{(z+1)^3 + 1} \right) \right)}{2(z+1) \left(3z - 2\sqrt{(z+1)^3 + 3} \right)}, \quad (33)$$

$$z_r = y,$$

which is defined for non-negative z except when $L(z) = 0$ at $z = 5/4$, which corresponds to $R_z = 0$ as can be seen from (10). Curve $J + Ky = 0$ of the system (33) can be attractive like on the first quarter of the phase plane when L and K are negative and J is positive, which occurs at range $5/4 < z < 65/16$, assuming $H_0 > 0$. A situation of this kind is illustrated in Fig. 2. The case in the figure does not show any signs of attractivity: it seems that at the

range $5/4 < z < 65/16$ none of the flow arrows below the curve $J + Ly = 0$ would lead any solutions towards it. This deduction is strengthened by (31), which (by assuming $H_0 > 0$) in this case reduces to be:

$$g_m(z) = 30 \left(\sqrt{\frac{(z+1)^5 (7339 - 8z(64z^2 - 516z + 963))^2}{(65 - 16z)^6}} + \frac{8(z(112z - 883) + 1192)(z+1)^3}{(16z - 65)^3} \right) < \frac{\delta_y}{H_0}, \quad (34)$$

where the subscript m marks that this is the explicit form of the function $g(z; \Omega_i)$ in the dust filled case. At the range $5/4 \leq z \leq 65/16$ the function $g_m(z)$ is monotonically increasing from zero to infinity, which suggest that the nullcline $J + Ky = 0$ of the system (33) can hardly be attractive like throughout the gap $5/4 \leq z \leq 65/16$.

The left hand side portrait in Fig. 2 illustrates what happens close by $z = 5/4$, where the system (33) is not defined. Even a slightest variation from today's observed value of H_0 seems to lead to a very different kind of universe. It is notable, that numerical calculations do not give the same answers for Eqs. (33) and (32) even with $H_0 = 0.7$, since the solution of Eqs. (33) can not cross the point $z = 5/4$. The area where J is positive, and L and K are negative, does not seem attractive at all, and only very close to the singularity it might be attractive like according to $g_m(z)$.

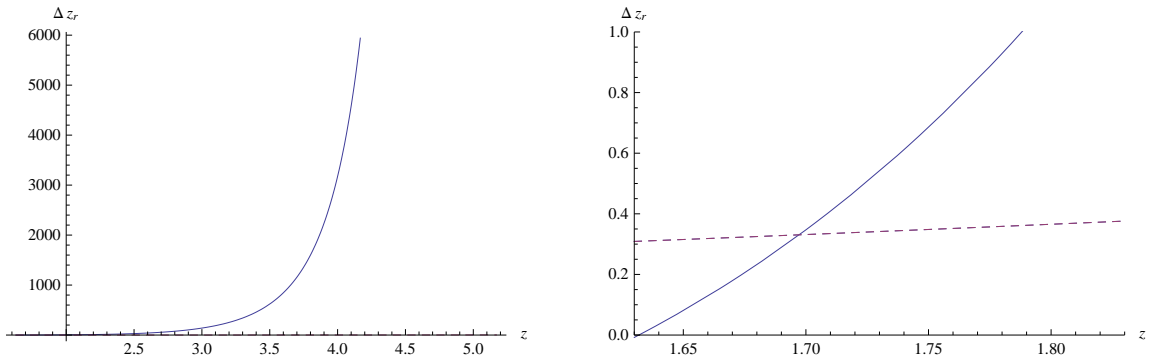


FIG. 3: Both functions, $g_{\Lambda m}$ and z_r^{oi} , can be interpreted as a difference between two z_r values, and are presented as such in a $(\Delta z_r, z)$ -plane. In both planes the solid curve is $g_{\Lambda m}$ and the dashed curve is z_r^{oi} . On the left hand side are $g_{\Lambda m}$ and z_r^{oi} drawn throughout the values of z where the nullcline can be attractive like, and on the right hand side are the same curves drawn at $1.63 < z < 2.00$. On the left hand side plot the scale of Δz_r is such, that in practice the dashed curve is indistinguishable from the z -axis. From the right hand side plot one can see that at what range of z values is δ_y/H_0 smaller than observational inaccuracies.

C. Dark energy and dust filled universe

Next we assume universe to be homogeneous, flat and consists of dust and dark energy, thus from Eq. (24) we obtain

$$z_r = H_0(z+1)\sqrt{(z+1)^3\Omega_m + \Omega_\Lambda}. \quad (35)$$

Quantity $R(z)$ takes now a very inelegant form, which also is the case in every function including $R(z)$, hence none of the functions including $R(z)$ is explicitly presented in this subsection. Also, $R(z)$ includes an elliptic integral of the first kind, which makes accurate algebraic analysis difficult. However, numerical methods are sufficient enough in this case.

Observations restrict the parameter values of this model: six-parameter Λ CDM model fit to WMAP nine-year data gives $\Omega_\Lambda = 0.721 \pm 0.025$, $\Omega_m = 0.279 \pm 0.025$, and $H_0 = 0.700 \pm 0.022^{20}$. From Eq. (35) can be seen, that the effect of dark energy with $\Omega_m = 0.279$, $\Omega_\Lambda = 0.721$ is less than one percent when $z \geq 5.37$, which is less than the inaccuracies of observed Ω_m , Ω_Λ , and H_0 values. Hence, at $5.37 \leq z$ we approximate this model model to have $\Omega_\Lambda = 0$. This approximation and numerical analysis at $0 \leq z \leq 5.37$ reveals, that $L(z) = 0$ only at $z \approx 1.63$, and L and K are negative and J is positive approximately at $1.63 < z < 5.18$. In this case the boundary condition (31) reduces to be of the form

$$\frac{\delta_y}{H_0} > g_{\Lambda m}(z; \Omega_\Lambda, \Omega_m), \quad (36)$$

where the subscript Λm marks that this is the function $g(z; \Omega_i)$ in the dust and dark energy filled case. The explicit form of the function $g_{\Lambda m}(z; \Omega_\Lambda, \Omega_m)$ is neither elegant nor necessary to show here, thus it is not presented here. At

$1.63 < z < 5.18$ the function $g_{\Lambda m}(z)$ is monotonically increasing, and it is increasing in a very rapid fashion (as can be seen from Fig. 3). In²⁰ are the values of Ω_Λ and Ω_m given with error margin ± 0.025 , so function

$$z_r^{oi} := \frac{|z_r(z; \Omega_\Lambda = 0.696; \Omega_m = 0.304) - z_r(z; \Omega_\Lambda = 0.746; \Omega_m = 0.254)|}{H_0} \quad (37)$$

represents the observational inaccuracy independent of parameter H_0 . From the portrait on the right hand side of Fig. 3 can be seen, that $g_{\Lambda m}(z) < z_r^{oi}$ at $1.63 < z < 1.70$, which therefore is the gap where this model can be attractive like.

The time period corresponding z values $1.63 - 1.70$ takes place about $9.70 - 9.85$ Gyr ago. Even though about 0.15 Gyrs could be enough time for universe to evolve into similar state everywhere, thus possibly explaining the observations done at some range of z values, it certainly can not explain the homogeneity of the observations at larger redshift values, *e.g.* over 10 Gyr old galaxies or CMB. The system with values $\Omega_m = 0.279$, $\Omega_\Lambda = 0.721$, and $H_0 = 0.700$ is illustrated on the right hand side on Fig. 2. The phase portrait looks similar to that of the dust filled case.

III. CONCLUSIONS AND DISCUSSION

Phase space analysis is used to find out if there is isotropic dust source models describing the universe without fine tuning the initial state. In general with inhomogeneous models, it is not always reasonable to use term initial state to refer only to the state of the system at Big Bang time, but sometimes also later times. This is due to observations: there is no observations of each location at all time during the entire history of the universe. The Big Bang might of occurred at different times in different regions, and the regions might of evolved completely differently compared to each other. Hence, here the term is not fixed to some particular time or place, but is rather determined for each case separately, whatever is most convenient for the situation. Often we use it to refer to the time relatively near in the past of each observable, but there are some exceptions, such as homogeneous case, which are discussed more later.

When cosmological observations are plotted on the (z_r, z) -plane, the curve that is the best fit to those plots is the curve we refer as the best fit curve. An cosmological observable to be observed in the vicinity of the best fit curve today, does not demand that the observable have to evolve towards the curve throughout its history; it only needs to be there when observed. A single observable could in principle move repeatedly towards and away from the curve during its entire history, as long as it locates close enough the curve when we observe it. Though the amount of observables basically eliminates this kind of excessive behavior, but a reasonable situation would be where each observable at some point approach the best fit curve and stay close enough before observed.

The interpretation of the dynamical equations simplifies in the case of homogeneous models, as the initial state is same everywhere and the Big Bang time occurred simultaneous everywhere; none of the quantities in equations governing the evolution are dependent of r , and the evolution have been similar always and everywhere. Thus, the minimum requirement for a FLRW metric based on model to be viable and stable enough is, that there has been a period where it have evolved towards the best fit curve and located inside boundaries given by observation inaccuracies since. This is the minimum requirement in the sense, that there was at least one early period where the best fit curve was attractive. The given example of the dust and dark matter filled case have an era where redshift is approaching the best fit curve: about $9.70-9.85$ Gyrs ago. Hence the model could explain almost the last 10 Gyrs.²⁵ Thus the model can not explain oldest observations. This is not surprising: as it is well known, without inflation homogeneous models have a fine tuning problem of matter and energy density.^{4,5} In the light of this paper, the stability is not a inbuilt feature at least in the cases studied in this paper, and can not replace the widely excepted solution of early time inflation for the fine tuning problem.

Analogous results are expected for almost homogeneous cases, where initial state does not vary too much with respect to r and the evolution can be thought of almost similar everywhere: observations can be explained without fine tuning the initial values, if at some point in the history before CMB there was a period where the universe evolved towards the best fit curve (and have been close enough it since). Thus we can conclude, that if the observed universe have not had a period in its history before CMB where the boundary condition we gave is satisfied, LT model can not explain its homogeneous nature without fine tuning.

The redshift values where the system is not defined, singular limits, causes difficulties for analysis. In this paper singular limits are not studied, and it is left to forthcoming publications. Nevertheless, one note of singular limits should be brought out here. In fig. 2 is illustrated what happens close by $z = 5/4$, where the system is not defined. Even a slightest variation from today's observed value of H_0 seems to lead a solution into very different direction at the singular limit. On the other hand, if we would of drawn the phase plane with *e.g.* $H_0 = 0.71$, the solution with $H_0 = 0.71$ would of approached towards point $\sim (1.25, 5)$ and the solutions with $H_0 = 0.70$ and $H_0 = 0.69$ would of approached towards the z -axis. This may be a sign, for example, of an instability of the model or of a break down

of the used method at this z value and its close neighborhood. As singular limits in general, also this phenomena is planned to be investigated thoroughly later.

The overall view our analysis cast on inhomogeneous models is not very promising. The best fit curve that should be attractive like is approximately given with Eq. (35), thus increasing at rate $z^{5/2}$ with large z values, and rapid increase of the curve makes it more unlikely to be attractive like. The situation seems to get worse if pressure is taken into account, since the increasing rate is then proportional to z^3 with large redshift. However, it is possible for observationally acceptable inhomogeneous (and therefore also homogeneous) models to be attractive like even with large z values, hence it needs to be investigated. The situation, however, is not necessarily as bad as it looks, since even though pressure at first seems to make the situation worse, it may actually recover it. This is due to the chances pressure brings with it to the evolution equation. For example, if the evolution equation changes from second order differential equation to higher order one, it may chance the structure of the stability of the system dramatically. This may even happen for homogeneous models, thus the result here received for dust and dark energy filled universe should not be interpreted as final.

-
- ¹ A. G. Riess et al., *Astron. J.* 116, 1009 (1998); *Astron. J.* 117, 707 (1999).
² S. Perlmutter et al., *Astrophys. J.* 517, 565 (1999).
³ D. N. Spergel et al. [WMAP Collaboration], (astro-ph/0603449).
⁴ E. W. Kolb, M. S. Turner, *The Early Universe*, Addison-Wesley (1994).
⁵ S. Weinberg, *Cosmology*, Oxford University Press (2008).
⁶ S. Weinberg, *The Cosmological Constant Problems*, (astro-ph/0005265).
⁷ M. F. Shirokov and I. Z. Fisher, *Isotropic Space with Discrete Gravitational-Field Sources. On the Theory of a Nonhomogeneous Isotropic Universe*, *Soviet Ast.* (1963) 6, 699.
⁸ T. Buchert, *On average properties of inhomogeneous fluids in general relativity. I: Dust cosmologies*, *Gen. Rel. Grav.* 32 (2000) 105 (arXiv:gr-qc/9906015).
⁹ G. Lematre, *Annales Soc. Sci. Brux. Ser. I Sci. Math. Astron. Phys. A* 53 (1933) 51. For an English translation, see: G. Lematre, *The Expanding Universe*, *Gen. Rel. Grav.* 29 (1997) 641.
¹⁰ R. C. Tolman, *Effect Of Inhomogeneity On Cosmological Models*, *Proc. Nat. Acad. Sci.* 20 (1934) 169.
¹¹ H. Bondi, *Spherically Symmetrical Models In General Relativity*, *Mon. Not. Roy. Astron. Soc.* 107 (1947) 410
¹² K. Bolejko, A. Krasinski, C. Hellaby, and M.-N. Celerier, *Structures in the Universe by Exact Methods*, Cambridge university press (2010).
¹³ N. Mustapha, C. Hellaby, and G.F.R.Ellis *Large-scale inhomogeneity versus source evolution: can we distinguish them observationally?*, *Mon. Not. R. Astron. Soc.* **292**, 817-830 (1997).
¹⁴ T. Mattsson, *Acceleration of the Cosmological Expansion as an Effect of Inhomogeneities*
¹⁵ N. Mustapha, B.A.C.C. Bassett, C. Hellaby, and G.F.R.Ellis *The Distortions of the Area Distance-Redshift Relation in Inhomogeneous Isotropic Universes*, *Class. Q. Grav.*, 15:2363-79, 1998, (arXiv:gr-qc/9708043v2).
¹⁶ T. Hui-Ching Lu, C. Hellaby *Obtaining the space time metric from cosmological observations.*, *Class. Q. Grav.*, 24:4107-31, 2007. (arXiv:0705.1060v2 [gr-qc]).
¹⁷ S. H. Strogatz *Nonlinear dynamics and chaos : with applications to physics, biology, chemistry, and engineering*, Addison-Wesley Publishing Company (1994)
¹⁸ I. Percival *Introduction to dynamics*, Cambridge University Press (1982)
¹⁹ S. Weinberg *Gravitation and cosmology : principles and applications of the general theory of relativity*, Wiley (1972)
²⁰ G. Hinshaw, D. Larson, E. Komatsu, D. N. Spergel, C. L. Bennett, J. Dunkley, M. R. Nolta, M. Halpern, R. S. Hill, N. Odegard, L. Page, K. M. Smith, J. L. Weiland, B. Gold, N. Jarosik, A. Kogut, M. Limon, S. S. Meyer, G. S. Tucker, E. Wollack, E. L. Wright *NINE-YEAR WILKINSON MICROWAVE ANISOTROPY PROBE (WMAP) OBSERVATIONS: COSMOLOGICAL PARAMETER RESULTS* (arXiv:1212.5226v1 [astro-ph.CO])
²¹ We consider the special case of the model where the observer is at the origin.
²² We use units in which $c = 1$.
²³ The number density of sources in redshift distance means the amount of sources per steradian per unit redshift interval.
²⁴ Note that here $\hat{\rho} = \frac{\mu n z r}{R^2}$ is already substituted into the null Raychaudhury equation.
²⁵ Since we do not have a general method to determine if an observable locates close enough the best fit curve when it is not attractive, we can not say if it really is so. So far the only way to determine this is to examine each case separately.